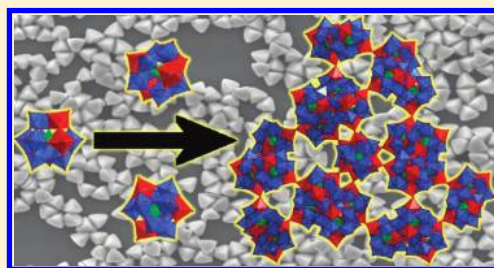


# Insights into the Self-Assembly Mechanism of the Modular Polyoxometalate “Keggin-Net” Family of Framework Materials and Their Electronic Properties

Johannes Thiel, Pedro I. Molina, Mark D. Symes, and Leroy Cronin\*

WestCHEM, School of Chemistry, The University of Glasgow, Glasgow G12 8QQ, U.K.

**ABSTRACT:** The mechanism for the syntheses of inorganic framework materials based solely on polyoxometalate Keggin clusters has been examined and their electronic properties have been investigated. The assembly of the modular network compounds with the molecular formula  $(C_4H_{10}NO)_n[W_{72}M_{12}O_{268}X_7]$  (with the heteroatom  $X = Si$  or  $Ge$  and the heterometal  $M = Co(II)$  or  $Mn(III)$ ) is based on the isomerization of the metastable precursor material  $[\gamma-XW_{10}O_{36}]^{8-}$ , followed by the inclusion of the heterometal and subsequent assembly into the extended framework structure. The two frameworks featuring manganese substitution can be dis- and reassembled in a recrystallization process while the cobalt versions do not show comparable behavior. The intrinsic differences of the four compounds with regards to their heteroatom and heterometal substitution are shown in terms of their redox behavior.



## INTRODUCTION

Research into modular inorganic framework materials, such as coordination polymers<sup>1–4</sup> and zeolites,<sup>5–7</sup> is one of the major fields in modern chemistry. These compounds find wide applications in different areas, such as catalysis,<sup>8,9</sup> gas sorption and purification<sup>10,11</sup> and ion-exchange.<sup>10,12</sup> Both compound classes show a high degree of structural variability, but while the purely inorganic zeolites stand out due to their tremendous stability,<sup>13</sup> the functionalization of metal-organic frameworks through their organic building blocks is much easier.<sup>14</sup> Polyoxometalates (POMs), molecular metal oxide clusters of early transition metals, such as molybdenum, vanadium, tungsten, etc.,<sup>15,16</sup> are prime candidates for secondary building units (SBUs) as they can potentially combine both these important features; stability and ease of functionalization. Their structural versatility and modularity<sup>16,17</sup> provide the foundation for their use as SBUs, which allows for potential insight into the reaction mechanisms,<sup>18</sup> while their diverse properties, for example, their redox-properties,<sup>19,20</sup> could be used to impart increased functionality to frameworks, leading to possible synergistic effects.

A diverse range of POM-based framework materials has been discovered over the past decade and various approaches have been employed to embed POMs into network structures.<sup>21–24</sup> Most of these methods rely on employing organic ligands<sup>25</sup> or transition metals<sup>23</sup> as additional linkers or on embedding the POM clusters directly into known framework structures.<sup>26</sup> More recently, we presented several examples of unprecedented POM framework structures,<sup>27–29</sup> where the metal oxide building blocks are directly connected without the use of external linkers. These isostructural compounds show high modularity: the tungsten-based Keggin clusters feature a heteroatom in the center that can either be silicon or

germanium, and heterometal substituents, which are either cobalt or manganese centers (see Figure 1a). This gives access to four different compounds with the overall formula  $[W_{72}M_{12}O_{268}X_7]^{n-}$  (with  $X = Si(IV)$  or  $Ge(IV)$ ,  $M = Mn(III)$  or  $Co(II)$ , and  $n = 40$  or  $52$ , respectively).<sup>27–29</sup> Additionally, it has been shown that the heterometals can be mixed in different ratios to form molecular alloys with emergent properties,<sup>29</sup> giving rise to an even wider range of compounds.

The framework structure features Keggin clusters that act as trigonal and tetrahedral nodes, assembling in a germanium nitride-like structure (see Figure 1). The trigonal building blocks are connected to three tetragonal nodes, which are then connected to four trigonal nodes and so on. They are linked by sharing corner oxo ligands of  $[WO_6]$  and  $[MO_6]$  octahedra of neighboring cluster units, resulting in  $M-O-W$  linkages to form the extended network structure. Morpholinium cations, which are employed during the synthesis, potentially have a templating effect and they act as counterions to stabilize the anionic framework; they are disordered in large cavities in the crystal structure which are comprised of rings of ten Keggin clusters, capped by two additional building blocks on either side.

It has been shown that the Keggin cluster-based framework materials exhibit extraordinary properties in terms of their solid state redox behavior.<sup>27–29</sup> All four compounds undergo reversible single crystal to single crystal (SCSC) transformation upon reduction or oxidation of the heterometal centers, which results in a color change and an alteration in the  $M-(O)-W$  distance and the length of the unit cell edge of the cubic

Received: October 9, 2011

Revised: December 1, 2011

Published: December 16, 2011

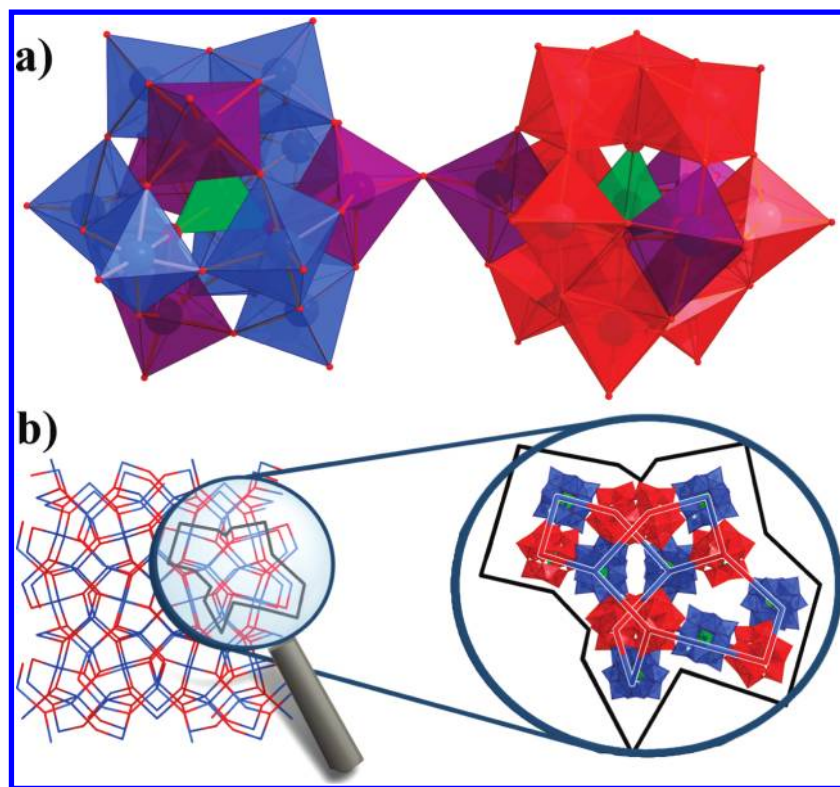


**Figure 1.** Graphical representation of (a) modularity of four- (blue) and three-connected (red) building blocks where the heteroatom  $\{XO_4\}$ -tetrahedra (with  $X = Si$  or  $Ge$ ) are shown in green and the heterometal  $\{(M/W)O_6\}$ -octahedra (with  $M = Mn$  or  $Co$ ), which connect to the neighboring Keggin clusters, are represented in purple. Statistically, only half of these metal positions are occupied by the heterometal, the other 50% are occupied by  $W$ . (b) Arrangement of the Keggin clusters into the three-dimensional framework on the left with a magnified representation of the distorted ten-membered ring, capped with two cluster units on either side.

framework.<sup>27–29</sup> The manganese centers, which occur in oxidation state (III) in the native materials, can be reduced to  $Mn(II)$  by suspending the crystals in methanol or acetonitrile using different types of hydrazines, quinoles or ascorbic acid. The reoxidation can be performed in a similar set up by treating the reduced crystals with *m*-CPBA, different quinones or hydrogen peroxide. Regarding the  $Co(II)$ -substituted frameworks, the initial oxidation is somewhat more difficult as  $Co(III)$  is highly unstable in hexaaqua complexes, to which the coordination environment in the POM frameworks is comparable.<sup>30</sup> However, by using a vast excess of *m*-CPBA, it is possible to retain the cobalt centers in the higher oxidation state for long enough to confirm the visually observed SCSC transformation by UV–vis spectroscopy and single crystal X-ray diffraction.<sup>29</sup>

Another striking feature of these materials is the option of recrystallizing the framework, which has been shown with the example of the manganese-substituted, silicon-centered Keggin cluster network.<sup>27</sup> The (at room temperature) insoluble compounds can be dissolved in boiling water and then recrystallized to give the original framework upon cooling. If the reduced,  $Mn(II)$ -containing version of the compound is dissolved in water, it recrystallizes in the native form after autoxidation of the heterometal centers.

These unique framework materials based on manganese and cobalt-substituted Keggin clusters represent a new class of compounds in the field of POMs and framework materials and they have given rise to novel and unusual properties. In an attempt to understand these properties and to develop a rationale for the mechanism of the formation of these three-

dimensional cluster assemblies, the syntheses of these compounds were optimized, taking knowledge about the solution behavior of POMs and especially of the lacunary clusters into account.<sup>31–33</sup> Furthermore, we herein present investigations of the electrochemistry of the Keggin frameworks by cyclic voltammetry in the solid state and solution phase and additional experiments on the recrystallization of these compounds.

## EXPERIMENTAL SECTION

All commercially available reagents and solvents were purchased from Sigma Aldrich Chemical Co., Ltd., and Fisher Scientific. Unless otherwise stated, the materials were used without further purification. Precursors  $K_8[\gamma-SiW_{10}O_{36}] \cdot 12H_2O$ <sup>34</sup> and  $K_8[\gamma-GeW_{10}O_{36}] \cdot 6H_2O$ <sup>35</sup> were synthesized according to literature procedures.

**Optimized Syntheses of Native Keggin Cluster-Based Framework Materials.** Syntheses for  $(C_4H_{10}NO)_nH_m[W_{72}M_{12}X_7O_{268}]$  (with  $X = Si$  or  $Ge$ ;  $M = Mn(III)$  or  $Co(II)$ ,  $n = 40$  or  $46$ , and  $m = 0$  or  $6$ , respectively) have been published elsewhere before,<sup>27–29</sup> but these methods suffered from low reproducibility. The following synthetic procedures are the outcome of a series of experiments where the systematic variation of reaction parameters led to high reproducibility and high yields.

**Optimized Synthesis of  $(C_4H_{10}NO)_{40}[W_{72}Mn^{III}_{12}Si_7O_{268}] \cdot 48H_2O$  (1).** Morpholine (45.0 g, 517 mmol) was added to 1 L of 1 M aqueous NaCl solution, and the pH was subsequently adjusted to 8.0 using 4.5 M  $H_2SO_4$  (~45 mL). At this point, fresh air-dried  $K_8[\gamma-SiW_{10}O_{36}] \cdot 12H_2O$  (7.50 g, 2.52 mmol) was added and the reaction was stirred vigorously for one day.  $MnSO_4 \cdot H_2O$  (635 mg, 3.76 mmol) was subsequently added as a solid resulting in a bright yellow solution. The solution was then stirred for another hour.  $KMnO_4$  (120 mg, 0.760 mmol) was then added and the solution was stirred for a further 30 min. The deep brown solution was

filtered through filter paper to remove any precipitate. It was then split into five different 250 mL conical flasks and left to crystallize. Brown, tetrahedral crystals started to form after a few days. Yields varied from 200 to 400 mg with an average of 255 mg (11.2  $\mu\text{mol}$ ; 16.1% based on W).

Analysis was in accordance with the published literature.<sup>27</sup>

**Optimized Synthesis of  $(\text{C}_4\text{H}_{10}\text{NO})_{40}[\text{W}_{72}\text{Mn}^{\text{III}}_{12}\text{Ge}_7\text{O}_{268}]\cdot 48\text{H}_2\text{O}$  (2).** Morpholine (45.0 g, 517 mmol) was added to 1 L of 1 M aqueous NaCl solution and the pH was subsequently adjusted to 8.0 using 4.5 M  $\text{H}_2\text{SO}_4$  (~45 mL). At this point, fresh air-dried  $\text{K}_8[\gamma\text{-GeW}_{10}\text{O}_{36}]\cdot 6\text{H}_2\text{O}$  (7.30 g, 2.51 mmol) was added and the reaction was stirred vigorously for 4 h.  $\text{MnSO}_4\cdot\text{H}_2\text{O}$  (635 mg, 3.76 mmol) was subsequently added as a solid resulting in a bright yellow solution. The solution was then stirred for another hour.  $\text{KMnO}_4$  (120 mg, 0.760 mmol) was then added, and the solution was stirred for a further 30 min. The deep brown solution was filtered through filter paper to remove any precipitate. It was then split into five different 250 mL conical flasks and left to crystallize. Brown, tetrahedral crystals started to form after a few days. Yields varied from 200 to 400 mg with an average of 306 mg (13.1  $\mu\text{mol}$ ; 18.9% based on W).

Analysis was in accordance with the published literature.<sup>28</sup>

**Optimized Synthesis of  $(\text{C}_4\text{H}_{10}\text{NO})_{46}\text{H}_6[\text{W}_{72}\text{Co}^{\text{II}}_{12}\text{Si}_7\text{O}_{268}]\cdot 68\text{H}_2\text{O}$  (3).** Morpholine (45.0 g, 517 mmol) was added to 1 L of 1 M aqueous NaCl solution and the pH was subsequently adjusted to 8.0 using 4.5 M  $\text{H}_2\text{SO}_4$  (~45 mL). At this point, fresh air-dried  $\text{K}_8[\gamma\text{-SiW}_{10}\text{O}_{36}]\cdot 12\text{H}_2\text{O}$  (7.50 g, 2.52 mmol) was added, and the reaction was stirred vigorously for one day.  $\text{CoSO}_4\cdot 7\text{H}_2\text{O}$  (1.30 g, 4.50 mmol) was subsequently added as a solid resulting in a purple solution. The solution was then stirred for another hour.  $\text{H}_2\text{O}_2$ -solution (30 vol. %, 12.5 mL) was then added, and the reaction mixture was stirred for a further 30 min. The deep brown solution was filtered through filter paper to remove any precipitate. It was then split into five different 250 mL conical flasks and left to crystallize. Purple, tetrahedral crystals started to form after a few days. Yields varied from 200 to 400 mg with an average of 277 mg (11.7  $\mu\text{mol}$ ; 16.8% based on W).

Analysis was in accordance with the published literature.<sup>29</sup>

**Optimized Synthesis of  $(\text{C}_4\text{H}_{10}\text{NO})_{46}\text{H}_6[\text{W}_{72}\text{Co}^{\text{II}}_{12}\text{Ge}_7\text{O}_{268}]\cdot 150\text{H}_2\text{O}$  (4).** Morpholine (45.0 g, 517 mmol) was added to 1 L of 1 M aqueous NaCl solution and the pH was subsequently adjusted to 8.0 using 4.5 M  $\text{H}_2\text{SO}_4$  (~45 mL). At this point, fresh air-dried  $\text{K}_8[\gamma\text{-GeW}_{10}\text{O}_{36}]\cdot 6\text{H}_2\text{O}$  (7.3 g, 2.51 mmol) was added, and the reaction was stirred vigorously for 4 h.  $\text{CoSO}_4\cdot 7\text{H}_2\text{O}$  (1.30 g, 4.50 mmol) was subsequently added as a solid resulting in a purple solution. The solution was then stirred for another hour.  $\text{H}_2\text{O}_2$  solution (30 vol. %, 12.5 mL) was then added, and the reaction mixture was stirred for a further 30 min. The deep brown solution was filtered through filter paper to remove any precipitate. It was then split into five different 250 mL conical flasks and left to crystallize. Purple, tetrahedral crystals started to form after a few days. Yields varied from 200 to 400 mg with an average of 295 mg (11.6  $\mu\text{mol}$ ; 16.7% based on W).

Analysis was in accordance with the published literature.<sup>29</sup>

**Electrochemistry.** Cyclic voltammetry (CV) was conducted in single compartment cells at room temperature in a three-electrode configuration using a Princeton Applied Research VersaSTAT 4 potentiostat. For solution CV, the compounds under investigation were dissolved in 0.1 M  $\text{Na}_2\text{HPO}_4$  (pH = 8.3) at a concentration of 1 mM. The scan rate was 0.1 V/s. The working electrode was a 3 mm diameter glassy carbon button electrode (BASi), the counter electrode was Pt wire and the reference electrode was Ag/AgCl (BASi). For solid state CV, solid samples of the compounds under investigation were deposited on the surface of the working electrode in a polystyrene matrix, as previously reported.<sup>29</sup> The supporting electrolyte was 0.1 M TBA- $\text{BF}_4$  (TBA = tetra-*n*-butylammonium) in acetonitrile. The scan rate was 0.1 V/s. The working electrode was a 3 mm diameter glassy carbon button electrode, the counter electrode was Pt wire and the reference electrode was Ag/AgNO<sub>3</sub> (BASi). Voltammograms for the solid-state studies are reported vs the

ferrocene/ferrocenium couple, determined by adding ferrocene to the supporting electrolyte (data not shown).

**Recrystallization of Compound 2.** Compound 2 (20 mg, 0.87  $\mu\text{mol}$ ) was heated in water (1 mL) at about 80 °C until completely dissolved; 80  $\mu\text{L}$  of this solution were drop casted onto ITO-glass (area ~1 cm<sup>2</sup>, Optical Filters Ltd.). The slide was left undisturbed and tetrahedral crystals formed overnight.

**Scanning Electron Microscopy.** Scanning electron microscopy was performed with a Philips XL30 ESEM instrument at an acceleration voltage of 25 kV. The sample was prepared by coating with a thin layer of gold deposited from a SC7640 sputter coater (VG Microtech).

## RESULTS AND DISCUSSION

**Mechanistic Considerations for an Optimized Synthesis of Keggin-Based Framework Materials.** Many repetitions of the syntheses of Keggin-based framework materials according to the procedures published<sup>27–29</sup> in the literature have highlighted the variable reproducibility of those methods. To overcome this problem, many experiments were conducted where the reaction conditions were varied, taking consideration of the possible mechanism for the framework assembly into account. The syntheses of the Keggin-based network materials can be divided into six basic steps, which then allow for simple modifications. In the ensuing discussion, these steps will be expounded and their significance and alterations compared to the previously described syntheses will be elucidated:

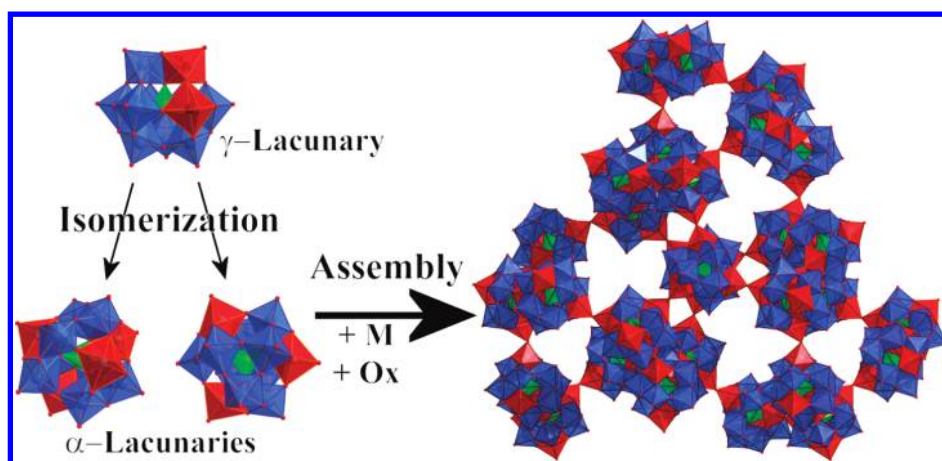
(i). *Syntheses of Precursor Materials  $\text{K}_8(\text{XW}_{10}\text{O}_{36})\cdot n\text{H}_2\text{O}$  ( $X = \text{Si}$  or  $\text{Ge}$ ;  $n = 12$  or  $6$ , respectively).* The syntheses of the precursors are based on well described literature procedures and require accurate pH control.<sup>34,35</sup> The utilization of the metastable  $\gamma$ -lacunary clusters seems obligatory as its isomerization is a key step in the syntheses of the unique framework materials and comparable precursors as alternatives, such as  $\alpha$ - and  $\beta$ -type Keggin clusters did not allow any analogous framework materials to be isolated.

(ii). *Preparation of the Reaction Medium.* The reaction medium is based on a morpholinium sulfate buffer in a 1 M aqueous sodium chloride solution. The ionic strength and buffer capacity of this mixture are crucial and the morpholinium cations act as counterions with a templating effect for the network structure.

(iii). *Addition of the Precursor  $\text{K}_8[\text{XW}_{10}\text{O}_{36}]\cdot 12\text{H}_2\text{O}$ .* A longer stirring time after addition of the precursor materials to the buffer solution reduced the crystallization time of the materials significantly and led to a higher reproducibility of the syntheses. This is especially important for the germanium-based networks where the time for the formation of the first crystals decreased from one month to approximately six days and the formation of the often observed byproduct ( $\text{Na}_4\text{K}(\text{C}_4\text{H}_{10}\text{NO})_7\{[\text{GeW}_9\text{O}_{34}]_2[\text{Mn}(\text{III})_4\text{Mn}(\text{II})_2\text{O}_4(\text{H}_2\text{O})_4]\}\cdot 15\text{H}_2\text{O}$ )<sup>37</sup> was completely prevented.

(iv). *Addition of the Transition Metal Salt  $\text{MSO}_4\cdot x\text{H}_2\text{O}$  ( $M = \text{Mn}$ ,  $\text{Co}$ ;  $x = 1$  or  $7$ , respectively).* Also in this case, an increase in stirring time led to a slight improvement in yields. No alternatives were found to successfully substitute for the sulfate versions of these salts.

(v). *Addition of the Oxidizing Reagent.* The addition of potassium permanganate for the manganese substituted POM frameworks is not crucial (as the manganese centers can undergo autoxidation), but it accelerates the crystallization process significantly. For the cobalt-based compounds on the other hand, hydrogen peroxide is needed to oxidize the

Scheme 1. Simplified Schematic Showing the Rationale for the Formation Mechanism of Keggin Cluster-Based Framework Materials<sup>a</sup>

<sup>a</sup>After the crucial initial isomerization of the  $\gamma$ -lacunary species and subsequent addition of the heterometal sulfate and oxidation, the clusters assemble into a three-dimensional framework.

transition metal to cobalt(III) during the framework synthesis, even though it is found in oxidation state (II) in the as-isolated native frameworks.

(vi). *Crystallization.* The first crystals usually appear within a few days when the solution is left in an open Erlenmeyer flask at 18 °C. If, however, about a third of the solution evaporates without any crystallization occurring, the vessel needs to be sealed to prevent precipitation of colorless materials. The germanium-centered lacunary clusters give faster formation of the desired products than the silicon-centered clusters do, and the manganese-substituted compounds crystallize faster than the cobalt versions.

The huge improvement regarding the reproducibility and yields for the syntheses, caused by the extension of the stirring time, indicates that the isomerization of the  $[\gamma\text{-XW}_{10}\text{O}_{36}]^{8-}$  precursor units to  $\alpha$ -type clusters is the critical step in the synthetic procedures (see Scheme 1). The framework materials solely consist of  $\alpha$ -Keggin building blocks and it has been discussed in the literature at length that this isomerization process can easily occur,<sup>34</sup> especially at the high pH value of eight where the reactions studied in this work take place. Various  $\alpha$ -isomers of some description ( $\{\text{XW}_{12-x}\text{Va}_x\}$ , Va = vacant position) are supposedly formed in complex dis- and reassembly processes, which allows subsequent substitution with the heterometals manganese or cobalt, after their addition. It is very likely that the isomerization still occurs after the addition of the transition metal sulfates, but it seems that the addition of the heterometals at an earlier stage hinders the formation of the  $\alpha$ -isomers and hence, the formation of the desired products (see Scheme 1).

It has also been found that an increased stirring time after addition of the transition metal improves the yield slightly. This does not seem to be as crucial as the increased reaction time for the isomerization of the lacunary clusters, but it helps to improve the outcome of the reaction in the form of increased yields. The oxidation of the heterometals is also very important for the syntheses of manganese- and cobalt-substituted Keggin-based framework materials. Both transition metals are originally added with their oxidation state being two, but whereas the manganese substituted frameworks finally crystallize containing manganese(III), cobalt experiences a re-reduction to cobalt(II)

after the initial oxidation. The addition of an extraneous oxidizing reagent is actually not an absolute necessity for the synthesis of manganese-based frameworks. The oxidation can also proceed *via* air oxidation, even though this increases the probability of the formation of the previously mentioned dimeric byproduct of germanium centered Keggin clusters connected by a manganese oxo double cubane, where only four of the six manganese centers are oxidized.<sup>36</sup>

On the other hand, the cobalt-based frameworks do not form at all without the addition of an oxidizer. Surprisingly, the oxidation to cobalt(III) is a fundamental step in the framework formation, although the heterometal has the oxidation state of (II) in the final network material. The reason for this might be the initial incorporation of cobalt centers into the vacant positions in the lacunary fragments; because of the low Lewis acidity of cobalt(II) ions, their coordination by the polyanion might not be sufficiently favorable.<sup>37</sup> Cobalt(III) ions on the other hand are classified as hard Lewis acids. This facilitates the initial interaction with the POM clusters and finally results in their incorporation. The re-reduction to cobalt(II) is a common phenomenon that has been observed before for  $[\text{Co}(\text{H}_2\text{O})_6]^{3+}$  and similar octahedral Co(III) complexes in aqueous solution.<sup>38</sup>

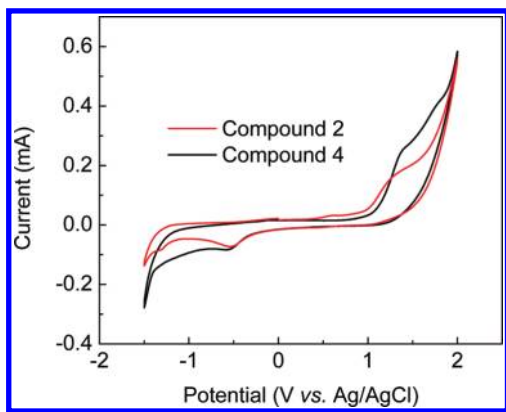
Furthermore, it has been observed that the germanium-centered Keggin clusters allow for a faster crystallization of framework materials than the silicon-based ones. The germanium versions also require a shorter stirring time, four compared to twenty-four hours, for the initial isomerization process, thus showing a lower stability than the silicon-centered lacunary clusters. Another important point for the synthesis of cobalt-substituted network materials is that the reduction of transition metals substituted into germanium-centered clusters is much easier than for silicon-centered ones. This has also been discussed previously in the literature.<sup>28,30</sup>

For the faster formation of manganese-substituted frameworks, there are again two possible reasons: the manganese(III) ions, as the harder Lewis acids,<sup>39</sup> form more stable complexes with the POM clusters than cobalt(II) ions. Alternatively, this could be because the manganese centers do not have to be re-reduced, before the framework can be formed, as they crystallize as manganese(III); unlike the cobalt-substituted

frameworks, which crystallize with cobalt(II) after initial oxidation to cobalt(III) and re-reduction.

**Electrochemistry.** To investigate the electronic properties of compounds 1–4, cyclic voltammetric measurements were performed in solution phase and the solid state.

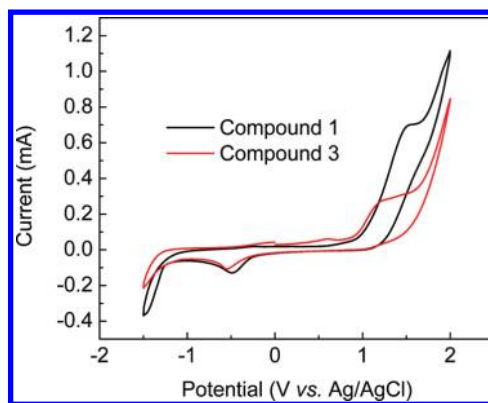
Figure 2 compares the cyclic voltammograms for compounds 2 and 4 dissolved in 0.1 M  $\text{Na}_2\text{HPO}_4$  at a concentration of 1



**Figure 2.** Comparison of solution CV measurements for compounds 2 and 4. The scan rate was 0.1 V/s. The working electrode was a 3 mm diameter glassy carbon button electrode, the counter electrode was Pt wire and the reference electrode was Ag/AgCl.

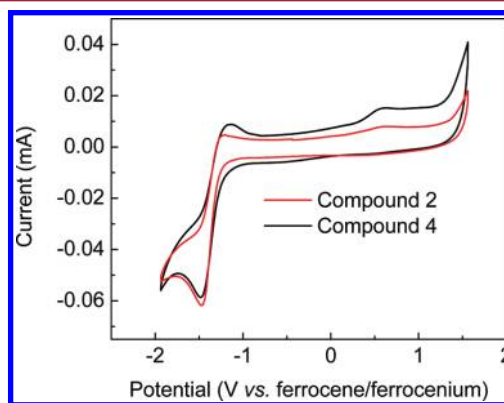
mM. In the cathodic direction, the tungsten reduction waves are not readily visible, and probably occur more negative than  $-1.5$  V (vs Ag/AgCl). However, it was not possible to scan this low, as any tungsten reduction waves would be obscured by the large wave associated with solvent breakdown. In the anodic direction, the cobalt substituted framework shows two shoulders against the large background of current from water oxidation. Both these oxidation events appear to be irreversible. The first oxidation wave occurs at  $+1.35$  V and is assigned to the oxidation of Co(II) to Co(III); the second process (at around  $+1.7$  V) is therefore most likely to be the oxidation of these Co(III) centers to Co(IV), which is in accordance with the position of the Co(III)/Co(IV) redox wave found in other water-soluble cobalt-oxo clusters.<sup>40,41</sup> In the case of manganese, there is only one broad oxidation process (also electrochemically irreversible), occurring around  $+1.25$  V (vs Ag/AgCl). This is likely to be the oxidation of Mn(III) to Mn(IV) as this wave is also observed on the first scan when scanning from 0 V to  $+2$  V (the initial redox state of the Mn in these compounds is (III)). Processes which could be ascribed to a possible Mn(II)/Mn(III) redox couple were not observed. The peaks at  $-0.5$  V in each of the voltammograms are due to oxygen created during scanning to  $+2$  V.

Figure 3 shows the comparison of the cyclic voltammograms of compounds 1 and 3 dissolved in 0.1 M  $\text{Na}_2\text{HPO}_4$  at a concentration of 1 mM. The results are similar to the ones for compounds 2 and 4: the oxidation processes are irreversible in all cases. However the Mn(III)/Mn(IV) wave is now shifted cathodically to  $+1.15$  V (vs Ag/AgCl), implying a thermodynamically easier oxidation of the manganese centers. The cobalt substituted framework on the other hand seems to behave in the opposite sense: the first wave is now at  $+1.50$  V vs Ag/AgCl (an anodic shift of 0.15 V for the putative Co(II)/Co(III) wave), while the second wave is no longer evident within the range scanned.



**Figure 3.** Comparison of solution CV measurements for compounds 1 and 3. The scan rate was 0.1 V/s. The working electrode was a 3 mm diameter glassy carbon button electrode, the counter electrode was Pt wire and the reference electrode was Ag/AgCl.

Figures 4 and 5 show the solid-state CVs of compounds 1 to 4. In all four traces, a tungsten reduction wave is visible at



**Figure 4.** Comparison of solid-state CV of compounds 2 and 4 in a polystyrene matrix. The scan rate was 0.1 V/s.

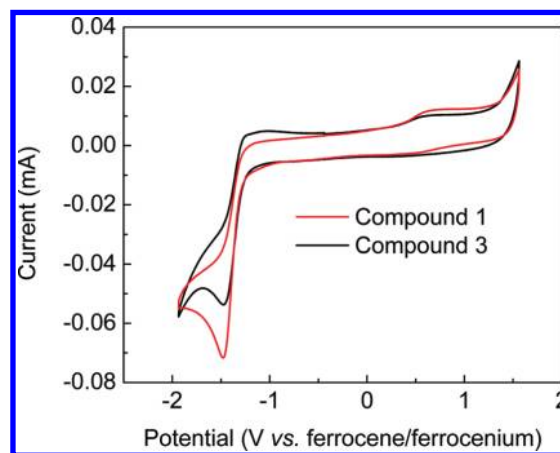


**Figure 5.** Comparison of solid-state CV of compounds 1 and 3 in a polystyrene matrix. The scan rate was 0.1 V/s.

$-1.40$  V versus ferrocene, and its position is invariant.<sup>42</sup> All four traces display broad, rather poorly resolved irreversible oxidation processes around  $+0.5$  V which probably correspond to the Co(II)/Co(III) and Mn(III)/Mn(IV) redox couples in their respective compounds. It is interesting to note that the putative Co(III)/Co(IV) wave observed in the solution phase

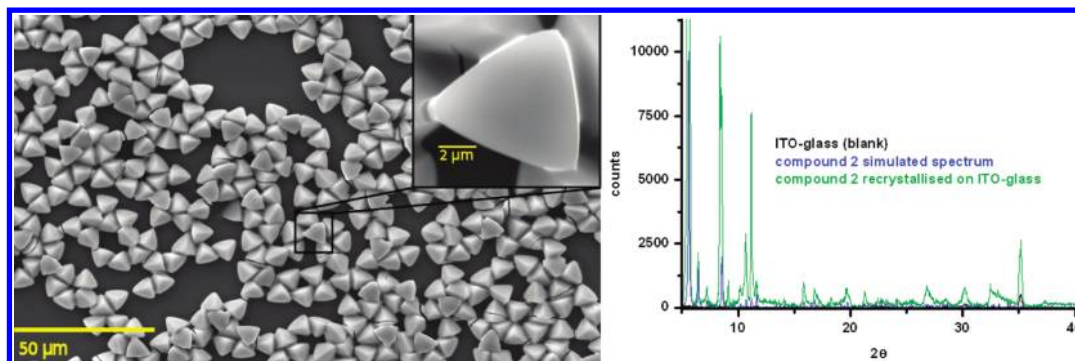


**Figure 6.** SEM image of crystals of compound 2, recrystallized on an ITO-slide (left) and the corresponding powder XRD spectra (right).

CVs is no longer evident in these solid state studies. This could be because the more rigid solid state framework structure prevents the alteration in the coordination environment of the cobalt centers necessary to establish such a high oxidation state. We also note that the HOMO–LUMO gap suggested by CV appears to be smaller in the solid state than in the solution-based CVs. This is consistent with a greater reorganization energy for the solvent environment in the solution-phase studies (aqueous 0.1 M  $\text{Na}_2\text{HPO}_4$ ) upon changing the charge of the clusters than for the less polar environment of the solid state CVs (polystyrene matrix and acetonitrile as solvent). Hence both oxidation and reduction are harder to achieve in the solution phase (greater solvent rearrangement occurs), giving a larger apparent HOMO–LUMO gap.

**Recrystallization.** As it has been shown before that compound 1 is an example of the few extended framework materials that can dis- and reassemble in a simple recrystallization process,<sup>27</sup> it should be possible to observe similar behavior with the other three isostructural Keggin cluster-based networks. Compound 2, the germanium-centered, manganese-substituted version of the framework materials, is soluble in hot water and it was possible to recrystallize it in the shape of tetrahedral crystals from a highly concentrated solution, shown in Figure 6.

However, many attempts to recrystallize the cobalt-substituted compounds 3 and 4 did not result in any success. This supports the hypothesis that the presence of Co(III) is necessary for the assembly of the extended framework materials. Compounds 3 and 4 contain only Co(II), and upon dissolution Co(III) cannot be generated. The addition of oxidizing reagents such as hydrogen peroxide after dissolution also did not lead to the formation of the tetrahedral crystals, most probably because the introduction of oxidizer and additional water shifts the solution equilibria unfavorably as regards the crystallization processes.

## CONCLUSIONS

We have successfully optimized the synthetic procedures for the formation of modular framework materials based on POM Keggin clusters. The solution properties of the precursors, the  $\gamma$ -lacunary clusters, have been exploited and because of our findings it can be reasoned that the isomerization of these precursors is the crucial step in the syntheses of the Keggin cluster-based network materials. Furthermore, we have shown how the choice of heterometal and heteroatom impacts on the syntheses and how it changes the overall properties of the frameworks in terms of their redox properties and autoreassembly from solution.

## AUTHOR INFORMATION

### Corresponding Author

\*Email: Lee.cronin@glasgow.ac.uk. Fax: (+44) 141-330-4888. Homepage: <http://www.croninlab.com>.

## ACKNOWLEDGMENTS

This work was supported by the EPSRC, the Leverhulme Trust, WestCHEM and the University of Glasgow and we thank Dr. Chris Ritchie and Dr. Carsten Streb for help with the initial synthesis and characterization of the Keggin-net materials and James Gallagher for help with SEM-measurements.

## REFERENCES

- Cheetham, A. K.; Férey, G.; Loiseau, T. *Angew. Chem., Int. Ed.* **1999**, *38*, 3268–3292.
- Eddaoudi, M.; Moler, D. B.; Li, H. L.; Chen, B. L.; Reineke, T. M.; O’Keeffe, M.; Yaghi, O. M. *Acc. Chem. Res.* **2001**, *34*, 319–330.
- Kitagawa, S.; Kitaura, R.; Noro, S. *Angew. Chem., Int. Ed.* **2004**, *43*, 2334–2375.
- Kitagawa, S.; Yanai, N.; Uemura, T.; Ohba, M.; Kadowaki, Y.; Maesato, M.; Takenaka, M.; Nishitsuji, S.; Hasegawa, H. *Angew. Chem., Int. Ed.* **2008**, *47*, 9883–9886.
- Davis, M. E.; Lobo, R. F. *Chem. Mater.* **1992**, *4*, 756–768.
- Corma, A. *Chem. Rev.* **1995**, *95*, 559–614.
- Corma, A. *J. Catal.* **2003**, *216*, 298–312.
- Kesanli, B.; Lin, W. B. *Coord. Chem. Rev.* **2003**, *246*, 305–326.
- Sayari, A. *Chem. Mater.* **1996**, *8*, 1840–1852.
- Férey, G. *Chem. Soc. Rev.* **2008**, *37*, 191–214.
- Janiak, C. *Dalton Trans.* **2003**, 2781–2804.
- Yaghi, O. M.; Li, G. M.; Li, H. L. *Nature* **1995**, *378*, 703–706.
- Zhang, Z. T.; Han, Y.; Zhu, L.; Wang, R. W.; Yu, Y.; Qiu, S. L.; Zhao, D. Y.; Xiao, F. S. *Angew. Chem., Int. Ed.* **2001**, *40*, 1258–1262.
- Ockwig, N. W.; Delgado-Friedrichs, O.; O’Keeffe, M.; Yaghi, O. M. *Acc. Chem. Res.* **2005**, *38*, 176–182.
- Long, D.-L.; Tsunashima, R.; Cronin, L. *Angew. Chem., Int. Ed.* **2010**, *49*, 1736–1758.
- Long, D.-L.; Burkholder, E.; Cronin, L. *Chem. Soc. Rev.* **2007**, *36*, 105–121.
- Ritchie, C.; Cooper, G. J. T.; Song, Y.-F.; Streb, C.; Yin, H. B.; Parenty, A. D. C.; MacLaren, D. A.; Cronin, L. *Nat. Chem.* **2009**, *1*, 47–52.
- Long, D.-L.; Streb, C.; Song, Y.-F.; Mitchell, S. G.; Cronin, L. *J. Am. Chem. Soc.* **2008**, *130*, 1830–1832.
- Mitchell, S. G.; Streb, C.; Miras, H. N.; Boyd, T.; Long, D.-L.; Cronin, L. *Nat. Chem.* **2010**, *2*, 308–312.
- Cronin, L.; Kögerler, P.; Müller, A. *J. Solid State Chem.* **2000**, *152*, 57–67.
- Mialane, P.; Dolbecq, A.; Sécheresse, F. *Chem. Commun.* **2006**, 3477–3485.
- Nohra, B.; Moll, H. E.; Rodriguez-Albelo, L. M.; Mialane, P.; Marrot, J.; Mellot-Draznieks, C.; O’Keeffe, M.; Biboum, R. N.;

Lemaire, J.; Keita, B.; Nadjo, L.; Dolbecq, A. *J. Am. Chem. Soc.* **2011**, *133*, 13363–13374.

(23) An, H.-Y.; Wang, E.-B.; Xiao, D.-R.; Li, Y.-G.; Su, Z.-M.; Xu, L. *Angew. Chem., Int. Ed.* **2006**, *45*, 904–908.

(24) Liu, S.; Xie, L.; Gao, B.; Zhang, C.; Sun, C.; Li, D.; Su, Z. *Chem. Commun.* **2005**, 5023–5025.

(25) Ruiz-Salvador, A. R.; Rodriguez-Albelo, L. M.; Sampieri, A.; Lewis, D. W.; Gomez, A.; Nohra, B.; Mialane, P.; Marrot, J.; Sécheresse, F.; Mellot-Draznieks, C.; Biboum, R. N.; Keita, B.; Nadjo, L.; Dolbecq, A. *J. Am. Chem. Soc.* **2009**, *131*, 16078–16087.

(26) Sun, C.-Y.; Liu, S.-X.; Liang, D.-D.; Shao, K.-Z.; Ren, Y.-H.; Su, Z.-M. *J. Am. Chem. Soc.* **2009**, *131*, 1883–1888.

(27) Ritchie, C.; Streb, C.; Thiel, J.; Mitchell, S. G.; Miras, H. N.; Long, D.-L.; Boyd, T.; Peacock, R. D.; McGlone, T.; Cronin, L. *Angew. Chem., Int. Ed.* **2008**, *47*, 6881–6884.

(28) Thiel, J.; Ritchie, C.; Streb, C.; Long, D.-L.; Cronin, L. *J. Am. Chem. Soc.* **2009**, *131*, 4180–4181.

(29) Thiel, J.; Ritchie, C.; Miras, H. N.; Streb, C.; Mitchell, S. G.; Boyd, T.; Ochoa, M. N. C.; Rosnes, M. H.; McIver, J.; Long, D.-L.; Cronin, L. *Angew. Chem., Int. Ed.* **2010**, *49*, 6984–6988.

(30) Tourné, C. M.; Tourné, G. F.; Malik, S. A.; Weakley, T. J. R. *J. Inorg. Nucl. Chem.* **1970**, *32*, 3875–3876.

(31) Hervé, G.; Tézé, A. *Inorg. Chem.* **1977**, *16*, 2115–2117.

(32) Tézé, A.; Hervé, G. *J. Inorg. Nucl. Chem.* **1977**, *39*, 2151–2154.

(33) Tézé, A.; Hervé, G. *J. Inorg. Nucl. Chem.* **1977**, *39*, 999–1002.

(34) Tézé, A.; Hervé, G. *Inorganic Syntheses*, Vol. 27; John Wiley & Sons: New York, 1990.

(35) Nsouli, N. H.; Bassil, B. S.; Dickman, M. H.; Kortz, U.; Keita, B.; Nadjo, L. *Inorg. Chem.* **2006**, *45*, 3858–3860.

(36) Ritchie, C.; Ferguson, A.; Nojiri, H.; Miras, H. N.; Song, Y.-F.; Long, D.-L.; Burkholder, E.; Murrie, M.; Kögerler, P.; Brechin, E. K.; Cronin, L. *Angew. Chem., Int. Ed.* **2008**, *47*, 5609–5612.

(37) Pearson, R. G. *J. Am. Chem. Soc.* **1963**, *85*, 3533–3539.

(38) Hollemann, A. F.; Wiberg, E. *Lehrbuch der Anorganischen Chemie*, 101 ed.; Walter de Gruyter: Berlin, 1995.

(39) Winter, M. J. *d-Block Chemistry*; Oxford University Press: Oxford, U.K., 1994.

(40) Symes, M. D.; Surendranath, Y.; Luttermann, D. A.; Nocera, D. G. *J. Am. Chem. Soc.* **2011**, *133*, 5174–5177.

(41) Gerken, J. B.; McAlpin, J. G.; Chen, J. Y. C.; Rigsby, M. L.; Casey, W. H.; Britt, R. D.; Stahl, S. S. *J. Am. Chem. Soc.* **2011**, *133*, 14431–14442.

(42) We note that in a previous study,<sup>29</sup> the tungsten waves of various compositions of these compounds were observed to vary from one another. In the present study, the CV measurements were commenced around +0.5 V vs ferrocene and scanned to +1.5 V vs ferrocene, before performing the negative portion of the scan. Hence in all cases, the irreversible oxidations observed over the range +0.5 V to +0.7 V vs ferrocene were performed before any reduction processes were probed. In our previous study, scans in the anodic direction only went as far as around +0.5 V vs ferrocene, and so these irreversible oxidation processes did not occur in these previous studies. Hence, in the current work, these irreversible oxidation processes may be causing structural changes to the compound which mean that the tungsten reduction potentials for compounds 1–4 are now more similar than in our previous study.